

Monitoring the Laser Metal Deposition (LMD) process by means of thermal methods

by E. D'Accardi*, F. Chiappini**, A. Giannasi**, M. Guerrini**, G. Maggiani**, D. Palumbo*, U. Galietti*

*Politecnico di Bari, Via Edoardo Orabona 4 – 70125 Bari BA, ester.daccardi@poliba.it, davide.palumbo@poliba.it, umberto.galietti@poliba.it

**Baker Hughes (BKR), Piazza Enrico Mattei – 50127 Firenze FI, Via Dorsale – 54100 Massa MS, federico.chiappini@bakerhughes.com, alessandra.giannasi@bakerhughes.com, massimo.guerrini@bakerhughes.com, gianluca.maggiani@bakerhughes.com

Abstract

Nowadays, Metal Additive manufacturing offers the advantages to build up components with good mechanical properties, complex shapes, and reduced times. However, the 3D manufacturing process is complex since it requires the simultaneous setting of different process parameters. For this reason, the production of components without defects requires the systematic use of non-destructive controls, offline or on-line, during the early stages of the process itself. Thermography can help in this sense, as a valuable tool to detect and quantify defects, using a simple experimental set-up consisting of a thermal sensor and excitation sources. In this work, novel procedures to analyse thermal data coming from the acquisition of different thermal sequences during the Laser Metal Deposition (LMD) process have been investigated and the capability of thermography to detect anomalies with the analysis of statistical indexes and thermal features has been evaluated. Furthermore, the possibility to correlate thermal features and process parameters has been demonstrated by means of an ANOVA analysis (Analysis of Variance) and regression models, considering experimental plans that involved the use of different parameters in terms of power, scanning speed and powder flow rate.

Introduction

Laser metal deposition (LMD) is an additive manufacturing process where a laser beam is used to melt a thin layer of the base material setting in a proper way the combination of different parameters. Generally, LMD process is used to produce and to repair high-value parts and components [1]. The process generates high-quality claddings and coatings with a lifetime of parts that partially extends their durability. This process is used for several applications and fields, oil and gas, aerospace, power generation, automotive and utilities industries.

A current challenge with LMD is that it is very difficult to predict the material and mechanical properties of produced components and coupons because there are different process parameters involved during the process [2]-[4]. In fact, the parts show very complex thermal behaviour, which depend on process variables and their combinations.

Furthermore, one of the main problems is to create components without localized or extensive defects and anomalies, such as porosity, and on the other hand, detects defects online, during the process itself and also offline by means of a suitable non-destructive controls [4]-[6].

Previous works have mainly used a visual-based control system with CMOS-, CCD-, or an infrared camera. Pyrometers and structured light scanning have also been used. Non-optical methods such as acoustical sensors and thermocouples have also been used for monitoring and control [2]-[5], [7]-[11]. In particular, the thermographic technique has already demonstrated its capability to control and predict the process and mechanical behaviour of coupons and components produced with other more established similar welding processes [12]-[14], but also more recently with AM processes [3]-[6].

In this work, an experimental approach has been used for investigating the LMD process by means of thermal methods, considering as main parameters the laser power, the scanning speed and the powder flow rate, to produce 26 coupons with the same geometry made of Inconel alloy IN718. Two identical microbolometer thermal sensors were adopted to monitor the process in two different positions, for a total of about 4500 acquired thermal sequences. One of these thermal sensors has been positioned integral with the laser scanning head and therefore it moved with at the same speed. The sensitivity of each extracted thermal feature was assessed by means of the ANOVA analysis with a statistical classical approach [10], [15], for different combinations of the process parameters. The analysis concerned the measurement of thermal features inside boxes and profiles. Then, polynomial regression models were adopted to describe the process parameter variation by means of the extracted thermal indexes. Furthermore, the analysis of the adopted thermal features has demonstrated the effectiveness of thermography as an on-line non-destructive control of the process, identifying anomalies and defects during the production of coupons.

Material and Methods

The material powder used in this work to produce 26 coupons was an Inconel alloy IN718. The production involved the analysis of 3 different levels for each parameter, for a total of 17 coupons and 9 replications, within a Design of Experiments (DOE) of the type 3³, with 3 main parameters laser power (P), scanning speed (v), powder flow rate (PFR)



and 3 different levels. Only 17 different coupons of the 27 available in a full factorial plan were produced because some combinations of parameters did not make the process stable. The analysis also regards combinations of the main process parameters indicated in Table 1 as Energy Density (ED) and Powder Flow Length (PFL) and defined as follows:

$$ED = \frac{P}{vD} \left[\frac{J}{mm^2} \right] \quad (1)$$

$$PFL = \frac{PFR}{v} \left[\frac{g}{mm} \right] \quad (2)$$

with D spot diameter, kept constant during the production of the different coupons. For the aim of the presented work, only the differences among the different levels have been considered for the analysis and indicated in Table 1. As it can be observed from Table 1, Level 2 is central to the extremes indicated as Level 1 and Level 3. To evaluate the replicability of the process and of the thermographic measurement, 9 coupons were produced twice, obtaining a complete experimental plan of the type 3² in which the main parameters were the energy density (ED) and the powder flow rate (PFR). Different subplans are also analysed by means of ANOVA to study the single and reciprocal influence towards a thermal monitoring of different features.

Input parameters	Laser Power (P) (kW)	Scanning Speed (v) (mm/min)	Powder Flow Rate (PFR) (g/h)	Energy Density (ED) (J/mm ²)	Powder Flow Length (PFL) (g/mm)
Levels	Level 1 = Level 2 – 0.35	Level 1 = Level 2 – 300	Level 1 = Level 2 – 200	Level 1	Level 1
	Level 2	Level 2	Level 2	Level 2	Level 2
	Level 3 = Level 2 + 0.35	Level 3 = Level 2 + 300	Level 3 = Level 2 + 200	Level 3	Level 3

Table 1. Scheme of the adopted DOE; main parameters laser power P, scanning speed (v), powder flow rate (PFR) and main combinations energy density ED, powder flow length PFL.

The adopted setup is reported in Figure 1, together with an example of the realized final coupon. The scanning strategy foresees 6 side-by-side passes and consecutive layers for a total length and height of about 150 mm. The two thermal sensors (FLIR A655sc indicated as 2 and 3 in Figure 1a) are microbolometer sensors in the range 7-14 μm, both used within the highest temperature range 200-3000 °C. A frame rate of 100 Hz was adopted to acquire the thermal data, while a subsampling at 25 Hz was necessary to analyse and compare the raw data at different laser scanning speed under the same conditions. In this work, the thermal data that come from the acquisitions related to the thermal sensor integral with the laser scanning head were analysed, described and discussed.

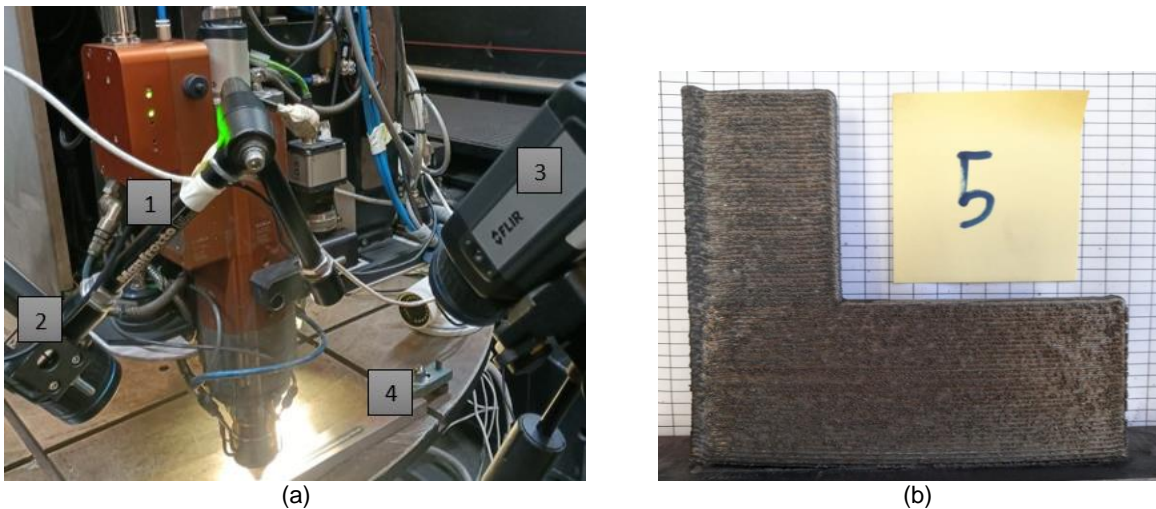


Figure 1. Experimental set-up (1) thermal source (laser head), (2-3) microbolometer sensors FLIR A655sc and (4) platform for the deposition; thermal technical specifications - frame rate 100 Hz, temperature range 300-2000 °C, window 640x120 pixels, spatial resolution integral sensor 0.25 mm/pixel (2), ~ 0.5 mm/pixel sensor in a fixed position (3).

Methodology and preliminary results

Figure 2 shows an example of the obtained thermal results, considering due different combinations of process parameters in terms of energy density, scanning speed and powder flow rate, but same input laser power (Level 2). In particular, Figure 2a shows an entire frame, considering all the pixels available within the thermal image, the apparent temperature, a central pass, halfway up the entire coupon created, or approximately at the end of the long side (Figure 1b). A zoom follows closer to the welding area, in which the Regions Of Interest (ROIs) chosen for the analysis are also

indicated, and in particular a rectangular box and a line profile, taken at the same height and distance from the molten pool (box – 35x13 pixels, vertical profile – 15 pixels). The maps shown in Figure 2b and 2c are related to two different coupons and so combination of different process parameters; for an immediate comparison they show the same scale. These results are only representative of the information that comes from the analysis of the thermal maps; for example, it is possible to observe how a lower thermal energy input corresponds into a more regular thermal print of the molten pool, and the powder results distributed equally. Similar results can be obtained considering the other coupons and the process parameters involved in these analyses; for brevity the other results are collected in the form of ANOVA analysis and regression models.

Different thermal features were extracted to carry out the ANOVA analysis, and in particular mean, standard deviation, mode, 98° percentile, 2° percentile, skewness, and kurtosis, related to the apparent temperature. In particular, for the analysis of the box, mean, standard deviation, mode, 98° percentile, 2° percentile are extracted, skewness and kurtosis along the y dimension, as different combinations of parameters demonstrated bimodal behaviour around the molten area (example in Figure 2a and 2b related to the same coupon). For the profile, all the analyses regarded the thermal data along y dimension. The analysis concerned for all the combinations of the process parameters the different six passes and three consecutive layers. Due to the adopted scanning strategy and involved process and thermal acquisition parameters, several data were available for each pass and layer. The data analyses were reduced considering a single data for each pass, and then obtaining 18 data that described each combination of parameters. These passages regarded the analysis of both boxes and profiles, with more than 100 ANOVAs as a result to be interpreted. After determining the statistical sensitivity of the different thermal features with the process parameters, simple polynomial models were adopted to describe the relationship thermal features and process parameters considering the three main process parameters power, scanning speed and powder flow rate and all the thermal features.

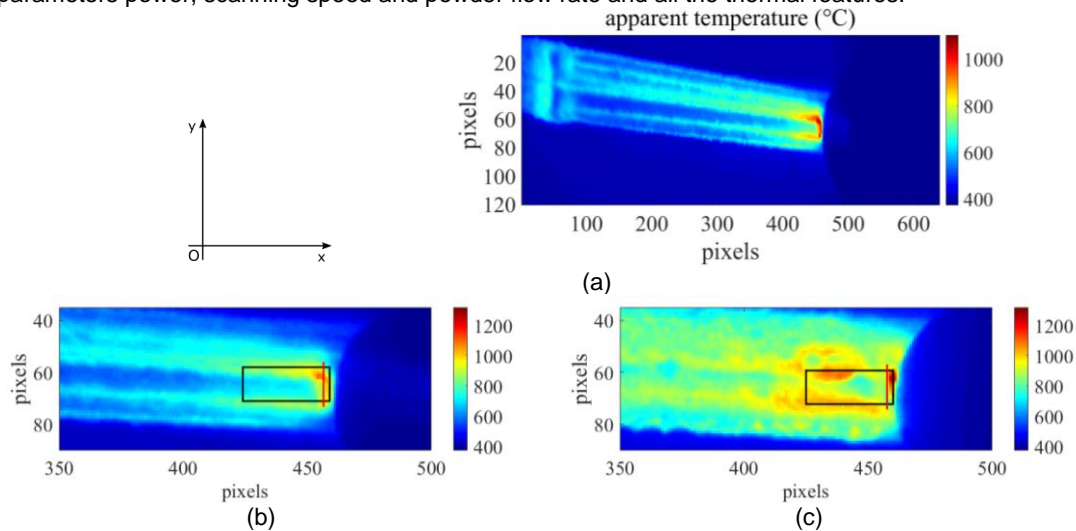


Figure 2. Example of the obtained thermal results; (a) coupon 12 – lower energy density level 1, scanning speed level 1, PFR level 3, (b) coupon 12 – lower energy density level 1, scanning speed level 3, PFR level 1, zoom, (c) coupon 16 – higher energy density level 3, scanning speed level 1, PFR level 3, zoom. The maps are related to the apparent temperature.

As comparison of the obtained results, Figure 3 shows an example of the trends related to different thermal features considering the box strategy, one passes (the first one), and the two combinations of parameters as already shown as maps related to a particular frame in Figure 2. In particular, Figure 3a is related to the standard deviation instead, Figure 3b shows the comparison in terms of mean, 2° and 98° percentile, comparing the same number of frames, at a frame rate of 25 Hz. The thermal trends related to the two different coupons are represented with two different colours, red for the coupon 12 and blue for the coupon 16. Higher energy density – coupon 16 results in higher apparent temperature (minimum, average and maximum) and in noise (standard deviation) that is also higher and less flat.

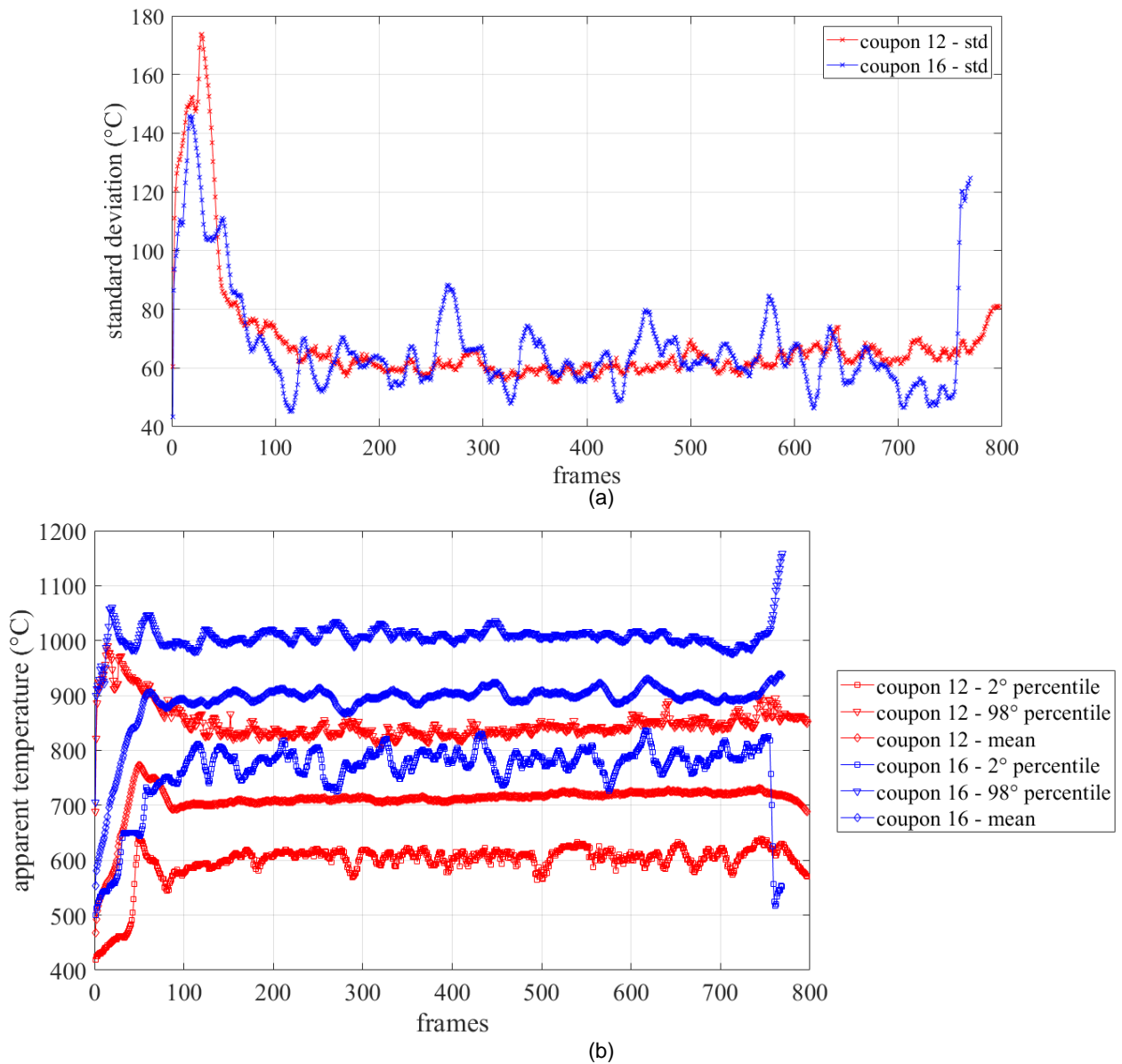


Figure 3. A comparison in terms of standard deviation (a), mean, 98° and 2° percentile (b) between two different coupons with two different combinations of parameters: coupon 16 – higher energy density level 3, scanning speed level 1, PFR level 3, coupon 12 – lower energy density level 1, scanning speed level 3, PFR level 1.

The reduction to a single data for each pass and then the analysis of subsequent layers with the aim to carry out regression models concerned only the data within the passes, avoiding the initial part of the coupon and the frames related to the phases during which the laser goes back after the various passes or at the end of a layer deposition. To have an idea of the data considered for each pass, Figure 4 shows an example in the case of profile analysis, where the various passes have been placed side by side and collected in a single map.

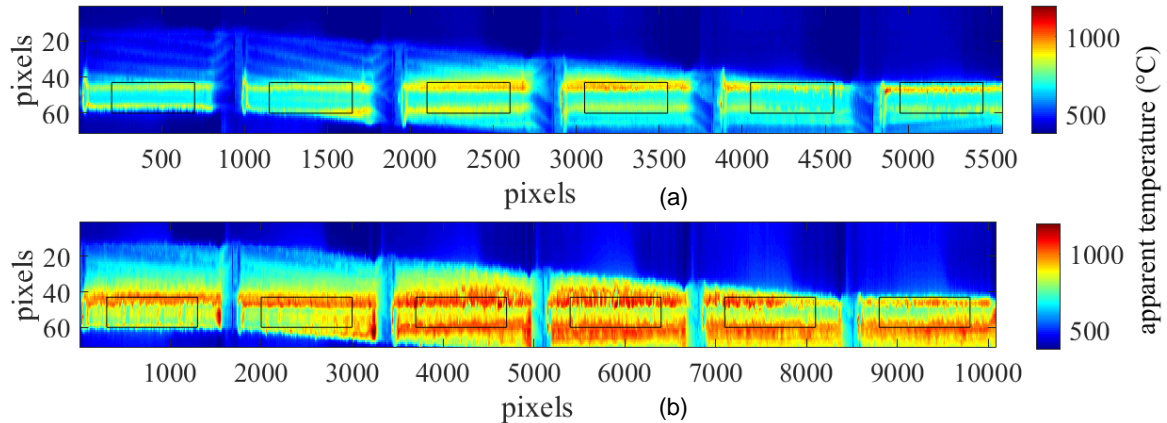


Figure 4. Maps of the thermal profiles placed side by side for each pass along an entire layer, (a) coupon 12 – lower energy density level 1, scanning speed level 3, PFR level 1, (b) coupon 16 – higher energy density level 3, scanning speed level 1, PFR level 3.

Results and discussion

In this section some results of the ANOVA analyses are reported, carried out for each coupon and combinations of process parameters. Only to be complete, ANOVA, which stands for Analysis of Variance, is a statistical test used to analyse the difference between the means of more than two groups. The null hypothesis (usually indicated with H_0) of ANOVA is that there is no difference among group means. The alternate hypothesis (H_a) is that at least one group differs significantly from the overall mean of the dependent variable. ANOVA determines whether the analysed groups associated with different levels and the independent variable are statistically different and so the p-value is equal to 0.

If any of the group means is significantly different from the overall mean, then the null hypothesis is rejected ($p\text{-value} > \alpha$ – in this work $\alpha=0.05$).

ANOVA uses the F-test for statistical significance. This allows for comparison of multiple means at once, because the error is calculated for the whole set of comparisons instead of each individual two-way comparison (that is the case of a t-test).

In particular, Table 2 summarizes the ANOVA analyses related to each coupon to determine the influence on the thermal response of some factors considered as replications.

Factors	Levels	Values	Responses
Passes	6	1, 2, 3, 4, 5, 6	Mean
Layers	3	1, 2, 3	98° percentile
Replications	2	1, 2	2° percentile
*** 2;3 -Way Interactions			Standard Deviation
			Kurtosis
			Skewness
			Mode

Table 2. ANOVA analysis carried out for each combination of parameters (17 coupons); analysed factors, levels, values and responses.

For some combinations of parameters and specific thermal features, the ANOVA analysis carried out to establish the influence of the data considered as replications such as passes, layers and print replications provided p-value equal to 0 or in any case less than 0.05 [10]. For this reason, in these cases, the data cannot be considered as actual replicas. This result can be intrinsic to the process (some combinations of parameters are in fact not optimal and, for example, require less or more powder as demonstrated also in some results shown below) or in any case in the thermographic measurements.

However, to consider this variability, all the data were considered to represent and describe in a proper way a set of process parameters and also to carry out other ANOVA analyses to establish the influence of a single process parameters or a combination of the same on the thermal response, or in other words, to determine the significance and sensitivity of each thermal feature in a statistical way. Tables 3 and 4 summarize the analyses, and describe the analyses carried out for the total experimental plan and for partial subplans in order to evaluate the statistical influence of the single process parameters and their combinations.

For all the cases and for almost all the thermal analysed features, considering both the strategy of the box and the profile, the result is always the same: the single variables and their combinations influence the thermal response with a p-value equal to 0. An example of the obtained result is reported below considering as thermal response the apparent mean temperature, the box strategy and the subplan described in Table 3.

Factors	Levels	Values	Responses
Energy Density (ED)	3	1, 2, 3	Mean
Powder Flow Rate (PFR)	3	1, 2, 3	98° percentile
*** 2 -Way Interactions			2° percentile
			Standard Deviation
			Kurtosis
			Skewness
			Mode

Table 3. ANOVA analysis carried out considering a partial experimental plan in which also the replications were taken into account; analysed factors, levels, values and responses.

Factors	Levels	Values	Responses
Power (P)	2 or 3	1, 2, 3	Mean
Scanning Speed (v)	2 or 3	1, 2, 3	98° percentile
Powder Flow Rate (PFR)	2 or 3	1, 2, 3	Mode
*** No Interactions for the complete experimental plan			2° percentile
** 2;3 -Way Interactions for subplans			Standard Deviation
			Kurtosis
			Skewness

Table 4. ANOVA analysis carried out considering the total experimental plan (it is not possible to evaluate the interactions because the plan is not complete and some combination of parameters were missed) and some subplans; analysed factors, levels, values and responses.

Factor Information						
Factor	Levels	Values				
ED	3	level 1; level 2; level 3				
PFR	3	level 1; level 2; level 3				
Analysis of Variance						
Source		DF	Adj SS	Adj MS	F-Value	P-Value
Model		8	416645	52081	197.18	0.000
	Linear	4	377327	94332	357.15	0.000
	ED	2	161226	80163	305.21	0.000
	PFR	2	216101	108051	409.09	0.000
	2-Way Interactions	4	39318	9829	37.22	0.000
	ED*PFR	4	39318	9829	37.22	0.000
Error		99	26148	264		
Total		107	442793			

Table 5. General Factorial Regression: Apparent Mean Temperature (°C) versus ED; PFR.

Considering the obtained results, it is possible to adopt an empirical model for describing the relationship between the process parameters and the thermal features. An approach in this sense will be show and explained below (Figure 5).

Model Summary					
S	R-sq	R-sq (adj)	R-sq (pred)		
26.4326	83.59%	83.12%	82.44%		
Coefficients					
Term	Coef	SE Coef	T-Value	P-Value	VIF
Constant	553.8	45.5	12.16	0.000	
ED	1.29	1.19	1.09	0.279	25.00
PFR	0.1699	0.0558	3.05	0.003	12.82
ED*PFR	0.00279	0.00145	1.92	0.058	36.82
Regression Equation					
App.Mean.Temp. = 553,8 + 1,29 ED + 0,1699 PFR + 0,00279 ED*PFR					

Table 6. Regression Analysis: Apparent Mean Temperature (°C) versus ED; PFR.

The only case for which the thermal response does not show a statistical significance is the one that considers the standard deviation as a thermal feature in correspondence to a change in the quantity of metal powder. The result of the ANOVA analysis in this case is reported below, considering the box strategy, and highlighting the not influence of the single powder factor but the statistical influence of the product energy density*powder.

Factor Information		
Factor	Levels	Values

ED	3	level 1; level 2; level 3				
PFR	3	level 1; level 2; level 3				
Analysis of Variance						
Source		DF	Adj SS	Adj MS	F-Value	P-Value
Model		8	16153.1	2019.13	59.66	0.000
	Linear	4	14624.6	3656.15	108.22	0.000
	ED	2	14520.8	7260.41	214.51	0.000
	PFR	2	103.8	51.88	1.53	0.221
	2-Way Interactions	4	1528.5	382.12	11.29	0.000
	ED*PFR	4	1528.5	382.12	11.29	0.000
Error		99	3350.8	33.85		
Total		107	19503.9			

Table 7. General Factorial Regression: Standard Deviation (°C) versus ED; PFR.

Similar results can be obtained considering the single parameters, and so the laser power, the scanning speed and the powder flow rate and the same thermal features. For this reason, also in this case, it is possible to describe the correlation between thermal features and process parameters with regression models that can be used for predicting the thermal behaviour of coupons printed with other process parameters. An example of these models is reported in Figure 5, choosing the apparent mean temperature as thermal feature and a polynomial model of second degree in which also the first-order interactions are considered:

$$thermal\ feature = Ax^2 + By^2 + Cz^2 + Dx + Ey + Fz + Gxy + Hxz + Iyz + L \quad (3)$$

that explaining all the terms becomes:

$$mean = 2.37e - 04P^2 - 106.01v^2 + 2.84e - 04PFR^2 + 0.22P + 235.90v - 0.45PFR + 0.26P * v + 1.02e - 05P * PFR + -0.17v * PFR + 764.75 \quad (4)$$

with a square correlation coefficient equal to $R^2 = 0.85$.

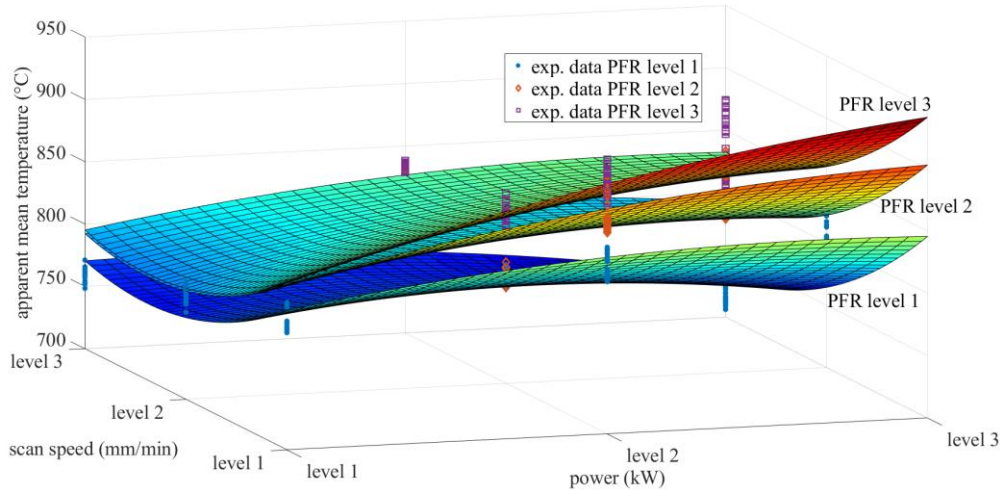


Figure 5. An example of the polynomial models used to describe the correlation thermal features – process parameters: apparent mean temperature vs laser power, scanning speed and powder flow rate.

Obviously, the obtained results are related to a certain position of the profile or alternatively of the box, position chosen immediately downstream of the fused area at a certain distance from the laser contour (about 10 pixels). The influence of the position, and box and profile dimensions, will be investigated in future works.

Considering the same thermal features and in particular the analysis of a profile, it is possible to highlight the presence of anomalies, or single defects that occur during the process and under certain process conditions. In Figure 6 is shown an example of the obtained results, considering the case of a trapped piece of powder falling during the deposition that produce a significant apparent temperature variation among different passes, in particular, those immediately following the occurrence of the unexpected defect.

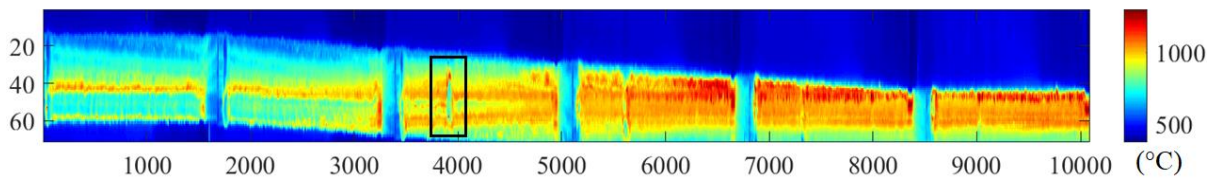


Figure 6. Example of the analysis of a thermal profile when an unexpected anomaly occurs during the process.

The presence of this anomaly is also evident from the analysis of the box and the trends associated with the different thermal features. An example is reported in Figures 7a and b, considering the apparent mean temperature before, during and after the anomaly for different passes and subsequent layers (Figure 7a). In Figure 7b are reported the maps related to different frames and therefore time instants during the deposition.

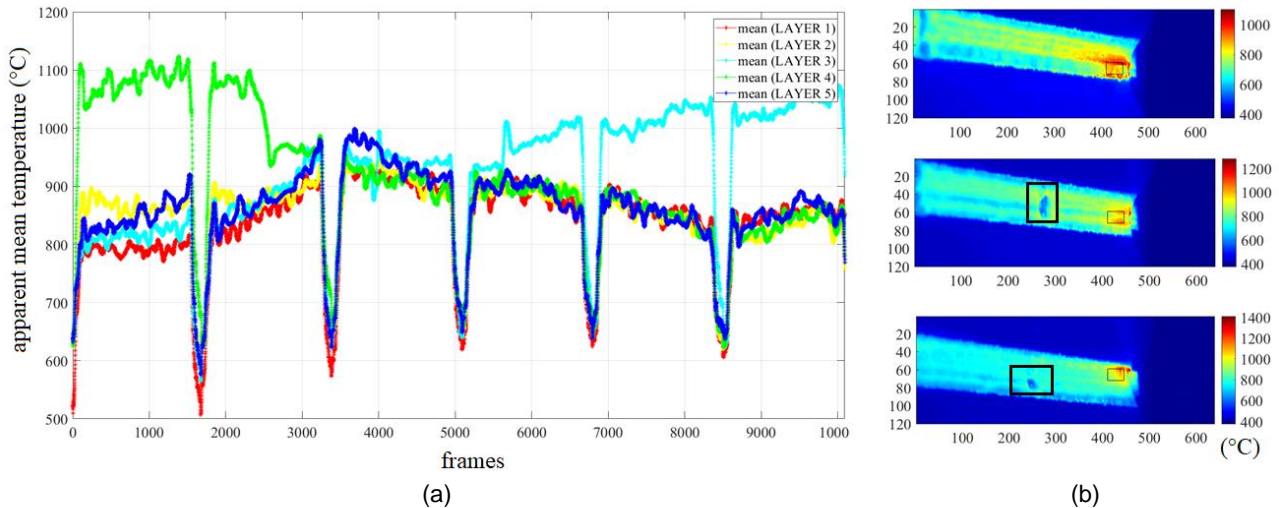


Figure 7. (a) Mean apparent temperature trends during the deposition when an unexpected anomaly occurs and (b) some significative frames.

The previous results confirm the effectiveness of thermal monitoring and of the features chosen to describe a precise set of process parameters. To confirm the presence of this defect during the deposition, simple macrographs were carried out, cutting the component produced in the section of interest identified during the thermal monitoring. The related result is shown in Figure 8.

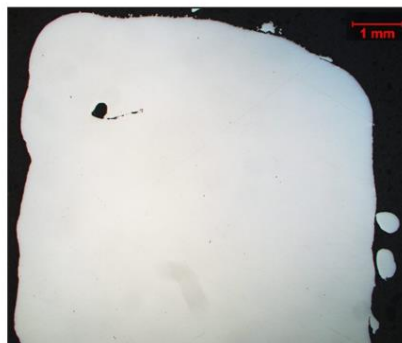


Figure 8. Macrograph which reveals the presence of an isolated anomaly detected in a non-destructive way thanks to thermal monitoring during the deposition of a coupon.

It is possible to check for similar or different anomalies (e.g. operator error in setting the laser scanning speed) adopting the profile strategy shown above. Some examples are shown below in Figure 9 and 10. The layers are indicated with a progressive number that indicates how they were acquired during the process by means of a thermal sensor and organized in groups of 5 layers to facilitate the acquisition, extraction, and subsequent analysis of the data. In particular, Figure 9 shows that is possible to detect the presence of a problem even before it occurs as a localized defect (there is no sufficient powder during the process), instead Figure 10 demonstrates how a problem can influence the subsequent passes and layers for a certain interval of time.

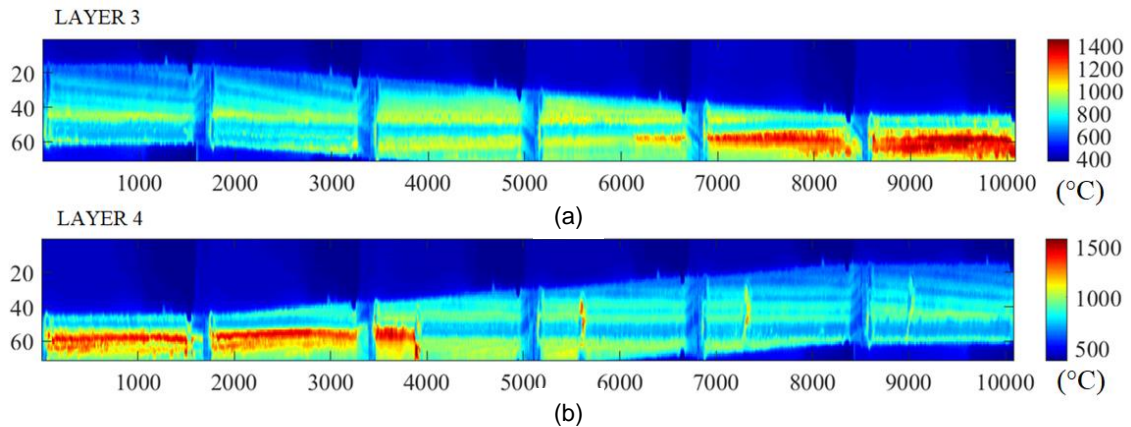


Figure 9. Presence of single anomalies during the process: it is possible to notice the presence of the defect (layer 4 – b) and even before (layer 3 – a) the need for more powder because probably the nozzle is worn out.

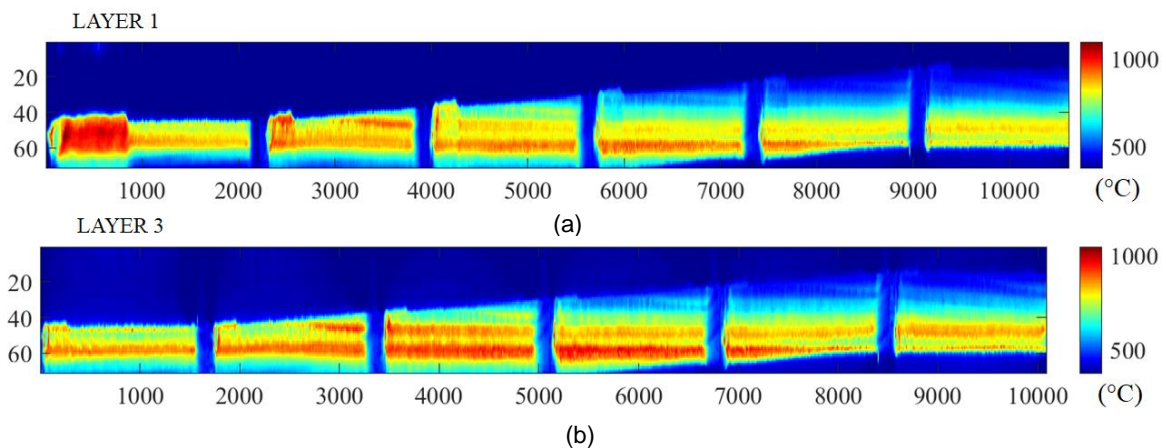


Figure 10. Presence of a localized anomaly due to an incorrect setting of process parameters in this case in terms of laser scanning speed (a) and how this problem influences the subsequent layers (b).

Conclusions

In this work the thermographic technique has been applied as an online control to monitor the LMD process during the production of different coupons in IN718 with the aim to correlate the thermal behaviour with the process parameters and to detect the presence of localized defects, in particular, process conditions. Several coupons were printed with different process parameters, adopting the same strategy, and following an experimental plan with three main factors and three levels. Different ANOVA analyses were carried out to establish the statistical influence of the process parameters on the thermal features and so the sensitivity of these thermal features for a robust monitoring. As thermal strategy used to describe the behaviours of the different coupons, two different ways were identified as useful and in particular the measure inside a box or a vertical profile. Different thermal features were considered as responses, and almost all showed a p-value equal to 0 when the process parameters changed. Simple polynomial models were adopted to describe the correlation between process parameters and thermal features, demonstrating the possibility of predicting the behaviour within the range investigated, with a R^2 greater than 0.8 (apparent mean temperature and mode). Finally, thanks to the analysis of the thermal profile, the presence of localized anomaly can be identified. This analysis is very effective as it can potentially reduce data acquisition and analysis times to a single profile, useful to describe the process parameter variation and the presence of a defect. Future works will also investigate the possibility to reduce the frame rate necessary during the acquisition and the data analysis for a robust online monitoring of large components, to guarantee a statistical mutual influence and a correlation between thermal and process behaviour. Furthermore, the statistical influence of the position of the box and of the profile was examined, revealing results consistent with the ones shown in this first work and that there will be the aim of future more extensive works.

References

- [1] Selcuk, C. (2013). Joining processes for powder metallurgy parts. In *Advances in powder metallurgy* (pp. 380-398). Woodhead Publishing.

- [2] Altenburg, S. J., Straße, A., Gumenyuk, A., & Maierhofer, C. (2020). In-situ monitoring of a laser metal deposition (LMD) process: Comparison of MWIR, SWIR and high-speed NIR thermography. *Quantitative InfraRed Thermography Journal*, 1-18.
- [3] Mazzarisi, M., Campanelli, S. L., Angelastro, A., Palano, F., & Dassisti, M. (2021). In situ monitoring of direct laser metal deposition of a nickel-based superalloy using infrared thermography. *The International Journal of Advanced Manufacturing Technology*, 112(1), 157-173.
- [4] Scheuschner, N., Altenburg, S. J., Gumenyuk, A., & Maierhofer, C. (2019). In-situ thermographic monitoring of the laser metal deposition process. In *Sim-AM 2019: II International Conference on Simulation for Additive Manufacturing* (pp. 246-255). CIMNE.
- [5] Altenburg, S. J., Straße, A., Gumenyuk, A., & Maierhofer, C. (2022). In-situ monitoring of a laser metal deposition (LMD) process: Comparison of MWIR, SWIR and high-speed NIR thermography. *Quantitative InfraRed Thermography Journal*, 19(2), 97-114.
- [6] D'Accardi, E., Krankenhagen, R., Ulbricht, A., Pelkner, M., Pohl, R., Palumbo, D., & Galietti, U. (2022). Capability to detect and localize typical defects of laser powder bed fusion (L-PBF) process: an experimental investigation with different non-destructive techniques. *Progress in Additive Manufacturing*, 1-18.
- [7] Jeon, I., & Sohn, H. (2022). Online melt pool depth estimation in laser metal deposition using a coaxial thermography system. *Journal of Laser Applications*, 34(2), 022001.
- [8] Hassler, U., Gruber, D., Hentschel, O., Sukowski, F., Grulich, T., & Seifert, L. (2016). In-situ monitoring and defect detection for laser metal deposition by using infrared thermography. *Physics Procedia*, 83, 1244-1252.
- [9] Li, L., Wang, X., & Huang, Y. (2021). Analysis of In Situ Optical Signals during Laser Metal Deposition of Aluminum Alloys. *Crystals*, 11(6), 589.
- [10] Mazzarisi, M., Errico, V., Angelastro, A., & Campanelli, S. L. (2022). Influence of standoff distance and laser defocusing distance on direct laser metal deposition of a nickel-based superalloy. *The International Journal of Advanced Manufacturing Technology*, 1-22.
- [11] Errico, V., Campanelli, S. L., Angelastro, A., Dassisti, M., Mazzarisi, M., & Bonserio, C. (2021). Coaxial Monitoring of AISI 316L Thin Walls Fabricated by Direct Metal Laser Deposition. *Materials*, 14(3), 673.
- [12] De Filippis, L. A. C., Serio, L. M., Palumbo, D., De Finis, R., & Galietti, U. (2017). Optimization and characterization of the Friction Stir Welded Sheets of AA 5754-H111: Monitoring of the quality of joints with thermographic techniques. *Materials*, 10(10), 1165.
- [13] Palumbo, D., De Finis, R., Serio, L. M., Galietti, U., & De Filippis, L. A. (2018, May). Thermographic signal analysis of friction stir welded AA 5754 H111 joints. In *Thermosense: Thermal Infrared Applications XL* (Vol. 10661, p. 106610Y). International Society for Optics and Photonics.
- [14] Serio, L. M., De Finis, R., & De Filippis, L. A. (2018, May). Capability of infrared thermography for studying the friction stir welding process. In *Thermosense: Thermal Infrared Applications XL* (Vol. 10661, p. 106610Z). International Society for Optics and Photonics.
- [15] Di Carolo, F., De Finis, R., Palumbo, D., & Galietti, U. (2019). A thermoelastic stress analysis general model: study of the influence of biaxial residual stress on aluminium and titanium. *Metals*, 9(6), 671.